NATIONAL ADVISORY COMMITTEE FOR AERONAUTICS

TECHNICAL NOTE 3900

INVESTIGATION OF VERTICAL DRAG AND PERIODIC AIRLOADS ACTING ON FLAT PANELS IN A ROTOR SLIPSTREAM

By Robert A. Makofski and George F. Menkick

Langley Aeronautical Laboratory
Langley Field, Va.

NACA

Washington
December 1956

B

NATIONAL ADVISORY COMMITTEE FOR AERONAUTI

TECHNICAL NOTE 3900

INVESTIGATION OF VERTICAL DRAG AND PERIODIC AIRLOADS ACTING ON FLAT PANELS IN A ROTOR SLIPSTREAM

By Robert A. Makofski and George F. Menkick

SUMMARY

Tests have been conducted on the Langley helicopter test tower to determine the vertical drag and pressure distributions acting on flat panels mounted normal to the rotor slipstream. The panels were tested with semispans of a rotor radius and of one-half a rotor radius at positions from 0.05 to 0.64 of a rotor radius beneath the plane of zero flapping.

Calculations of the vertical drag by use of a strip-analysis procedure outlined in this paper and the assumption of a fully contracted wake agreed well with the experimental results over the range from 0.20 to 0.64 rotor radius beneath the plane of zero flapping.

The pressure pulse caused by the passage of the blade over the panels is a maximum at about the 0.8 radius station. At this station, the pulse pressure decreases from 10 times the disk loading per blade at 0.05 radius beneath the plane of zero flapping to about one-half of the disk loading per blade at 0.64 radius beneath the plane of zero flapping.

No change in rotor power at constant rotor thrust was observed with the particular size or arrangement of the panels tested or even with the panels completely removed.

INTRODUCTION

The loss in available rotor thrust and the increase in aerodynamically induced vibration due to the positioning of such items as fuselages, wings, nacelles, and tails in the slipstream of a rotor has become of increasing importance with the advent of the convertiplane and the trend toward higher disk loadings for helicopters. The ability to determine the vertical drag and the periodic airloads acting on these items is necessary

if the designer is to obtain an accurate estimate of the performance of the aircraft and of the amplitude and frequency of the aerodynamically induced vibrations.

Reference 1 describes some initial data obtained to determine the loss in rotor static thrust due to a fixed surface located in the slipstream of the rotor. It was found that, for a flat panel extending the full rotor diameter at 0.33 and 0.67 of a rotor radius beneath the plane of zero flapping, the percent loss in rotor static thrust was roughly equal to 0.7 of the percent blocked disk area. No change in power due to the presence of the panel was observed, and no attempt was made to measure the periodic airloads.

The present investigation has been conducted to determine for a hovering rotor the accuracy with which the vertical drag on a flat panel in the slipstream of the rotor may be computed and to determine the magnitude and distribution of the periodic and the steady-state airloads acting on the panel. The flat panels used in this investigation are considered representative of wing surfaces. The drag coefficients of panels normal to an airstream are readily available. It seems plausible that, if the load on the panels can be computed with reasonable accuracy, the load on any shaped body can be similarly computed if the drag coefficient of that body is known.

The panels were tested with semispans of a rotor radius and of one-half a rotor radius. The area of the flat panels was 0.136 of the rotor disk area for the larger span and 0.068 of the disk area for the shorter span. The panels were tested at positions varying from 0.05 to 0.64 of a rotor radius beneath the plane of zero flapping and at rotor disk loadings of 1.36 and 2.36 lb/sq ft.

SYMBOLS

b	panel span, ft
B	number of blades
c	panel chord, ft
D	vertical drag of panels, lb
$p_u - p_a$	steady-state pressure between upper surface of panel and undisturbed atmospheric pressure, lb/sq ft
$p_u - p_l$	steady-state differential pressure between upper and lower surfaces of panel, lb/sq ft

$\Delta(p_u - p_a)$	pulse pressure referenced to atmospheric pressure, lb/sq ft
$\Delta(p_u - p_l)$	differential pulse pressure, lb/sq ft
r	radial distance, ft
R	rotor radius, ft
S	projected area of panels, lb/sq ft
T	rotor thrust (rotor shaft tension force), lb
z	distance beneath rotor plane of zero flapping, ft

APPARATUS

The Langley helicopter test tower is described in reference 2. The major modifications to the tower since the publication of reference 2 are an enlargement of the working area at the base of the tower and the replacement of the internal combustion engine by a 3,000-horsepower variable-frequency electric motor drive.

Rotor Blades

The helicopter rotor was a conventional two-blade rotor with flapping hinges located on the rotor shaft and with drag hinges located 12 inches from the center of rotation. The blades were of plywood construction and had a radius of 18.74 feet, an equivalent chord of 9.4 inches, a solidity of 0.027, no twist, and an NACA 23015 airfoil section. A view of the rotor blades and flat panels as mounted on the tower is shown in figure 1.

Flat Panels

The flat panels were made of plywood and were mounted normal to the rotor slipstream. A sketch of the flat panels and rotor is given in figure 2. The panels had a chord of 4 feet and were tested with semispans of a rotor radius and of one-half a rotor radius. Tests were made with the panels located at 1, 2, 3, 4, 6, 8, 10, and 12 feet beneath the plane of zero flapping.

Vertical-Load and Pressure Measurements

The average vertical load on the panels was measured by electrical strain gages mounted on the panel support as indicated in figure 2.

The pressures were measured by NACA miniature electrical pressure gages (ref. 3) located on one of the panels as indicated in figure 2. These gages were used to measure the differential pressure across the panel, that is, between the upper and lower surfaces, and also to measure the difference between the pressure on the upper surface and the undisturbed atmospheric pressure. The gages were located at spanwise stations of 30, 40, 50, 65, 80, 90, and 99.5 percent of the rotor radius and chordwise stations of 35, 50, and 85 percent of the chord. The signal from the pressure gage was recorded by an oscillograph.

METHODS AND ACCURACY

The test measurements were made at a wind velocity of zero and for steady-state operating conditions. The test procedure was to establish a constant rotor tip speed of 500 ft/sec and then to vary the disk loading through the desired range. Data were obtained at disk loadings of 0, 1.36, and 2.36 lb/sq ft. This procedure was repeated for each panel position and configuration.

The tests were conducted for ratios of panel area to rotor disk area of 0.136 for the large-span panels and 0.068 for the small-span panels.

ESTIMATED ACCURACIES

The estimated accuracies of the basic quantities measured in the test are as follows:

Rotor thrust, lb	±20
Rotor torque, ft-lb	±20
Rotor angular speed, rpm	± 1
Pressures, percent	± 5
Panel load, lb	± 4

The overall accuracy of the plotted results is believed to be ±3 percent except for the plotted pressure data which is believed to be within ±5 percent.

RESULTS AND DISCUSSION

The data obtained in this investigation have been analyzed in terms of the vertical drag of the panels and the steady-state and the periodic pressures acting on the panels. The vertical drag, which will be discussed first, has a direct bearing on the performance of the aircraft. The periodic airloads, discussed subsequently, can have an important effect on the aircraft vibration.

For a given rotor thrust and tip speed, no change in rotor power was observed for any of the panel configurations or positions tested or even with the panels removed. However, some "ground effect" could be expected if much larger panels were used.

Vertical Drag

The ratio of vertical drag to rotor thrust (which is taken as the tension in the rotor shaft) is presented in figure 3 as a function of the distance beneath the plane of zero flapping (nondimensionalized as z/R) for the two spans tested. The experimental points presented were taken from strain-gage measurements of the vertical drag at a disk loading of 2.36 lb/sq ft. Data taken at a disk loading of 1.36 lb/sq ft show excellent agreement with the results of figure 3. The short-span panel was not tested at distances of less than 0.2R from the plane of zero flapping.

On the large-span panel, the vertical drag decreases from 11 percent to 9.3 percent of the rotor thrust as the panel is moved from 0.05R to 0.2R beneath the plane of zero flapping. From 0.2R to 0.65R beneath the rotor, the vertical drag remains relatively constant at about 8.5 to 9 percent of the rotor thrust. This vertical-drag value corresponds to a loss in available rotor thrust of about 66 percent of the ratio of panel area to rotor disk area, which agrees reasonably well with the value of 0.70 cited in reference 1. For the small-span panels, the vertical drag averages about 2 percent of the rotor thrust for panel positions from 0.2R to 0.64R beneath the plane of zero flapping.

From the data available of this investigation, it appears that the vertical drag for panel positions from 0.2R to 0.64R will approximately follow the relationship

$$\frac{D}{T} = 0.66\left(\frac{S}{\pi R^2}\right)\left(\frac{b/2}{R}\right) \qquad (1)$$

The nonuniform variation of rotor induced velocity requires that a term, such as $\frac{b/2}{R}$, be included in equation (1) in order to predict the loading on panels having a span less than a rotor diameter. Additional data covering intermediate values of $\frac{b/2}{R}$ would be necessary to clarify the effect of wake contraction. The panel loading defined by equation (1) increases linearly with radial distance. Evidently, compensating errors are present when the equation is used inasmuch as data discussed subsequently show that the panel loading departs somewhat from a triangular distribution.

Vertical-drag calculations.- In order to calculate the vertical drag, it is necessary to take the rotor wake contraction into account. In this paper, the assumption is made that the rotor wake boundary is located at 75 percent of the rotor radius at a distance of 0.25R beneath the plane of zero flapping and that the wake is fully contracted at a distance of 0.60R beneath the plane of zero flapping. Furthermore, the assumption is made that the flow within the inboard 20 percent of the radius is negligible and that the air passing through this station proceeds downward with no change in spanwise station. This wake geometry is based on visual studies of the air flow using smoke together with wake-velocity studies previously made on the Langley helicopter test tower.

With these assumptions, the vertical drag of the panel can be computed by use of a strip-analysis procedure. This procedure is based on a computation of the induced velocities in the plane of the rotor. The distribution of dynamic pressure on the panels is obtained from this velocity distribution corrected for the wake contraction. The drag coefficients for a flat plate normal to a uniform flow were obtained from reference 4. Drag coefficients of 1.25 and 1.18 were determined for the large- and small-span panels, respectively. These coefficients are based on the aspect ratio of the panels and are assumed constant for stations along the panel.

The results of these calculations are given in figure 3. For the large-span panels, the calculation assuming a fully contracted wake is in good agreement with the experimental data at 0.6R beneath the plane of zero flapping. The vertical drag calculated by assuming an incomplete contraction to 0.75R at 0.25R below the plane of zero flapping is about 20 percent less than the experimental value. As will be discussed subsequently, this difference between the calculated and experimental values at panel positions near the rotor appears to be primarily due to the periodic airloads acting on the panel.

For the short-span panel, the calculation for $z/R = 0.6$ (wake fully contracted) predicts a vertical drag of about 30 percent above the experimental values, whereas the calculated drag for $z/R = 0.25$

(wake partially contracted) is 13 percent less than the experimental values. Although the percent discrepancy is large, the actual drag discrepancy as a fraction of the rotor thrust is very small; either assumption with regard to the wake contraction would give sufficient accuracy.

Spanwise center of loading.- The experimental center of loading for the large-span panel varied from 0.62R at 0.1R beneath the rotor to 0.53R at 0.65R beneath the rotor. For the short-span panel, the spanwise center of loading remained constant at about 0.42R over the range from 0.2R to 0.64R beneath the rotor plane of zero flapping. Centers of loading outboard of the panel midpoint are expected from a consideration of the spanwise distribution of induced velocity.

Pressure Distributions

The pressure measurements are of use in determining the steady-state and the periodic aerodynamic loading on the panels. Oscillograph records comparing the pressure-gage traces at disk loadings of 0 and about 2.3 lb/sq ft for the panels having a semispan of a rotor radius are presented in figure 4. Records are presented for various distances beneath the rotor plane of zero flapping. Measurements of the differential pressure, which represents the total loading on a panel, as well as the difference in pressure between the upper surface of the panel and the undisturbed atmospheric pressure are presented. The spanwise and chordwise location of the pressure gages are noted on the record.

The pressures acting on the panels are composed of a relatively steady-state component that exists in the wake between blade passages and a periodic component that occurs as each rotor blade passes over the panel. This periodic component is termed the pulse pressure.

The erratic behavior of the gages located at 0.9R and 0.995R appears to be due to the vortex from the rotor blade tip. This vortex can cause relatively large pressure fluctuations, as may be seen in figure 4(c). Experience has shown that the region influenced by the tip vortex will change with time even in a hovering condition inasmuch as the vortex shifts position in a random manner.

Pulse-pressure distribution.- The pulse pressure would be expected to increase with an increase in disk loading. At constant disk loading, an increase in the number of blades would be expected to decrease the pulse pressure. Close to the rotor (and for a constant disk loading and number of blades), an increase in blade chord would be expected to decrease the maximum pulse pressure. However, the time over which the pulse acts would be increased. Farther away, the pulse pressure would depend only on the blade lift. A pulse-pressure coefficient might then be defined as being the ratio of the pulse pressure to the blade lift or disk loading

per blade. Two methods are used in measuring the pulse pressures presented in this paper: In one method the pulse pressure is defined as the difference between the pressure on the upper surface of the panel and the undisturbed atmospheric pressure; in the other method it is defined as the differential pressure between the upper and lower surfaces of the panel.

In figure 5, the spanwise distribution of the pulse-pressure coefficient is plotted for distances from 0.05R to 0.64R beneath the rotor plane of zero flapping. The pulse-pressure coefficients utilizing both methods described previously are presented. Because of the erratic behavior of the pressure in the region of the blade tip, the pulse pressure as defined is not obtainable. In place of these pressures, the maximum and minimum pressure coefficients are presented, and dashed lines are used to represent these points.

The pulse-pressure coefficient referenced to undisturbed atmospheric pressure has a larger value than the differential pulse-pressure coefficient at the same station, although the fluctuation in pressure coefficient at the wing tip is somewhat greater for the differential-pressure reference. Both pulse-pressure coefficients are a maximum at about the 0.8R spanwise station. The spanwise distribution becomes more uniform as the distance beneath the rotor increases.

At $z/R = 0.05$ and 0.8R spanwise station, the pulse pressure, referenced to undisturbed atmospheric pressure, is 10 times the disk loading per blade. This value decreases rapidly until, at $z/R = 0.64$ and 0.8R spanwise station, the pulse pressure is about one-half of the disk loading per blade. These rather large periodic loads occurring at the blade-passage frequency point out the importance of avoiding fuselage or wing structural frequencies at or near the blade-passage frequency since this could lead to high vibration levels and fatigue failures. A similar discussion would apply to the differential pulse-pressure coefficients.

Steady-state-pressure distribution.- The steady-state pressure that acts on the panel between blade passages may be nondimensionalized by dividing the pressure by the disk loading to obtain the steady-pressure coefficient. In figure 6, plots are presented of the spanwise variation of the steady-pressure coefficient at 0.50c for distances from 0.05R to 0.64R beneath the rotor plane of zero flapping. The pressure is presented with reference to undisturbed atmospheric pressure and as the differential pressure between the upper and lower surfaces of the panel.

As in the case of the pulse pressure, the maximum steady-state pressure occurs near the 0.8R spanwise station and the pressure distribution tends to become more uniform as the distance beneath the rotor increases. This tendency agrees with the observation that the center of loading moves slightly inboard as the value of z/R is increased.

The maximum value of both steady-pressure coefficients is about equal and remains nearly constant at about 0.7 to 0.9 of the disk loading for the test range of values of z/R. The main effect of increasing z/R is to increase the pressure over the inboard regions with only negligible changes at the 0.8R spanwise station where maximum pressure occurs.

Relation of Periodic and Steady-State Pressures to Vertical Drag

The drag coefficients used in the strip-theory calculations discussed in the section entitled "Vertical-drag calculations" are for steady-state conditions and do not take into account the impulse acting on the panel. In an effort to explain the difference between the calculated and experimental values of the vertical drag given in figure 3, a spanwise integration of the steady-state pressure was performed and the area under the pressure pulses shown in the oscillograph records (fig. 4) was compared with the area under the steady-state pressure trace. The results indicate that, if only the steady-state pressures are integrated (assuming a uniform chordwise pressure distribution), the drag values are very similar to the calculated values of figure 3.

If the periodic loading is included, the vertical-drag values agree with the experimental strain-gage data in figure 3. This agreement may be shown in figure 7 which gives the ratio of the time average periodic loading to the steady loading as a function of the distance beneath the plane of zero flapping. The values presented represent the average value between the spanwise stations of 0.3R to 0.9R. At $z/R = 0.25$, the time-average periodic load is about 25 percent of the calculated loading. The total loading at $z/R = 0.25$ is then about 1.25 times the steady loading or about 9 percent of the rotor thrust. This value agrees with the experimental data of figure 3.

CONCLUSIONS

Tests have been conducted on the Langley helicopter test tower to determine the vertical drag and pressure distributions on panels mounted below a helicopter rotor and normal to the rotor shaft. The panels were tested with semispans of a rotor radius and of one-half a rotor radius and had areas of 0.136 and 0.068 of the rotor disk area, respectively. The panels were tested at positions from 0.05 to 0.64 of a rotor radius beneath the plane of zero flapping. Some of the more pertinent findings are as follows:

1. Calculations of the vertical drag by use of the strip-analysis procedure outlined in this paper and the assumption of a fully contracted wake agree well with the experimental results over the range from 0.20

to 0.64 of a rotor radius beneath the plane of zero flapping. For an accurate estimate of the vertical drag at distances of less than 0.2 of a rotor radius beneath the rotor plane of zero flapping, it is necessary to take into account the pulse pressure caused by the passage of the rotor blades over the panel.

2. From the data of this investigation, it appears that the ratio of vertical drag to rotor thrust for panel positions from 0.2 rotor radius to 0.64 rotor radius beneath the rotor plane of zero flapping is about 66 percent of the product of the ratio of panel area to rotor disk area and the ratio of panel semispan to rotor radius.

3. The pulse pressure is a maximum at about the 0.8 radius spanwise station. At this station, the pulse pressure decreases from 10 times the disk loading per blade at 0.05 radius beneath the rotor plane of zero flapping to about one-half of the disk loading per blade at 0.64 radius beneath the rotor plane of zero flapping.

4. The steady-state pressure, that is, the pressure in the wake between blade passages, is also a maximum at about the 0.8 radius station. Over the test range of distances beneath the rotor, the maximum pressure remained relatively constant at 0.7 to 0.9 of the disk loading.

5. For the test range of variables, no change in rotor power at constant rotor thrust was observed with changes in panel position or even with the panels completely removed.

Langley Aeronautical Laboratory,
National Advisory Committee for Aeronautics,
Langley Field, Va., September 20, 1956.

REFERENCES

1. Fail, R. A., and Eyre, R. C. W.: Loss of Static Thrust Due to a Fixed Surface Under a Helicopter Rotor. Tech. Note No. Aero.2008, British R.A.E., July 1949.

2. Carpenter, Paul J.: Effect of Wind Velocity on Performance of Helicopter Rotors As Investigated With the Langley Helicopter Apparatus. NACA TN 1698, 1948.

3. Patterson, John L.: A Miniature Electrical Pressure Gage Utilizing a Stretched Flat Diaphragm. NACA TN 2659, 1952.

4. Hoerner, Sighard F.: Aerodynamic Drag. Publ. by the author (148 Busteed, Midland Park, N.J.), 1951.

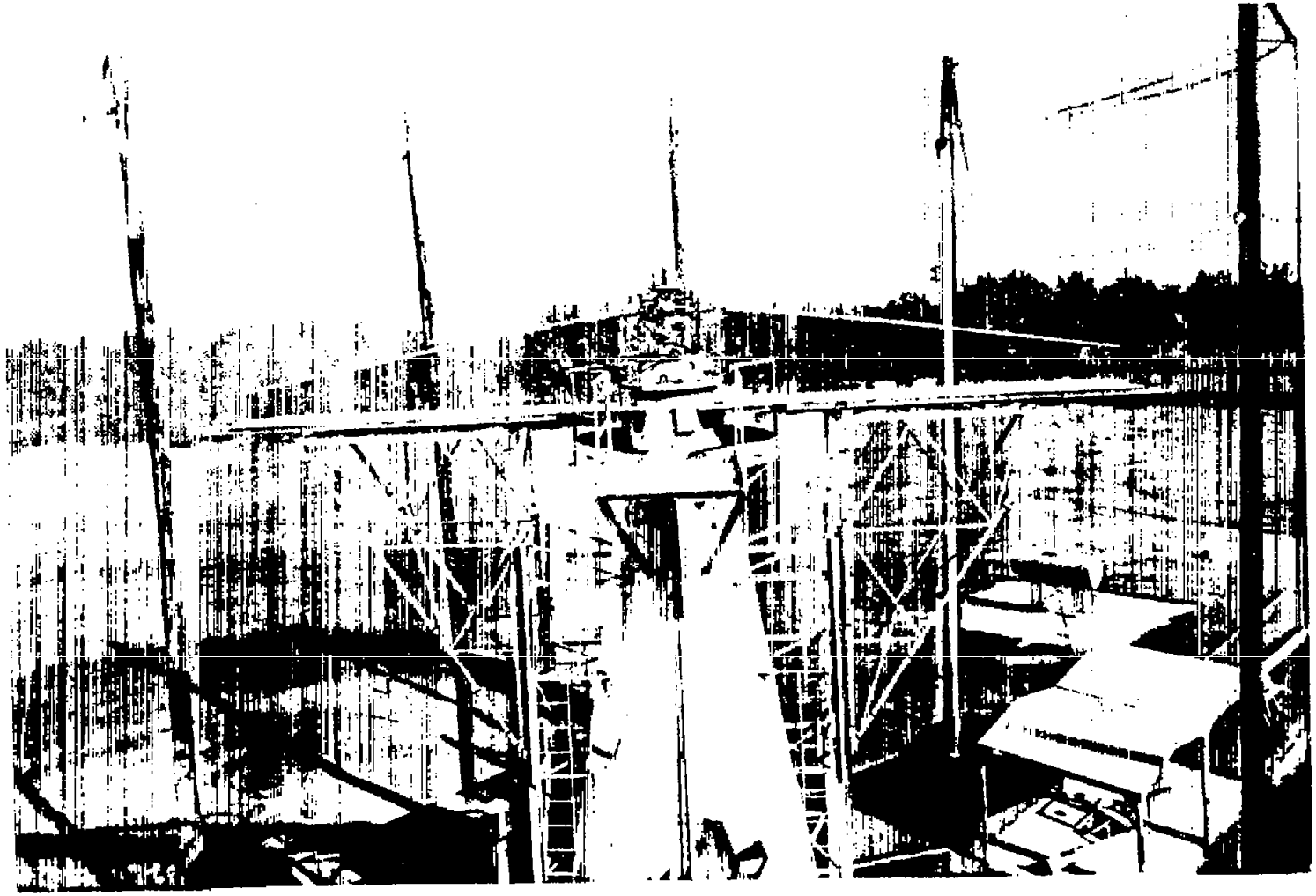

L-91054

Figure 1.- View of rotor and panels mounted on test tower; z/R = 0.21.

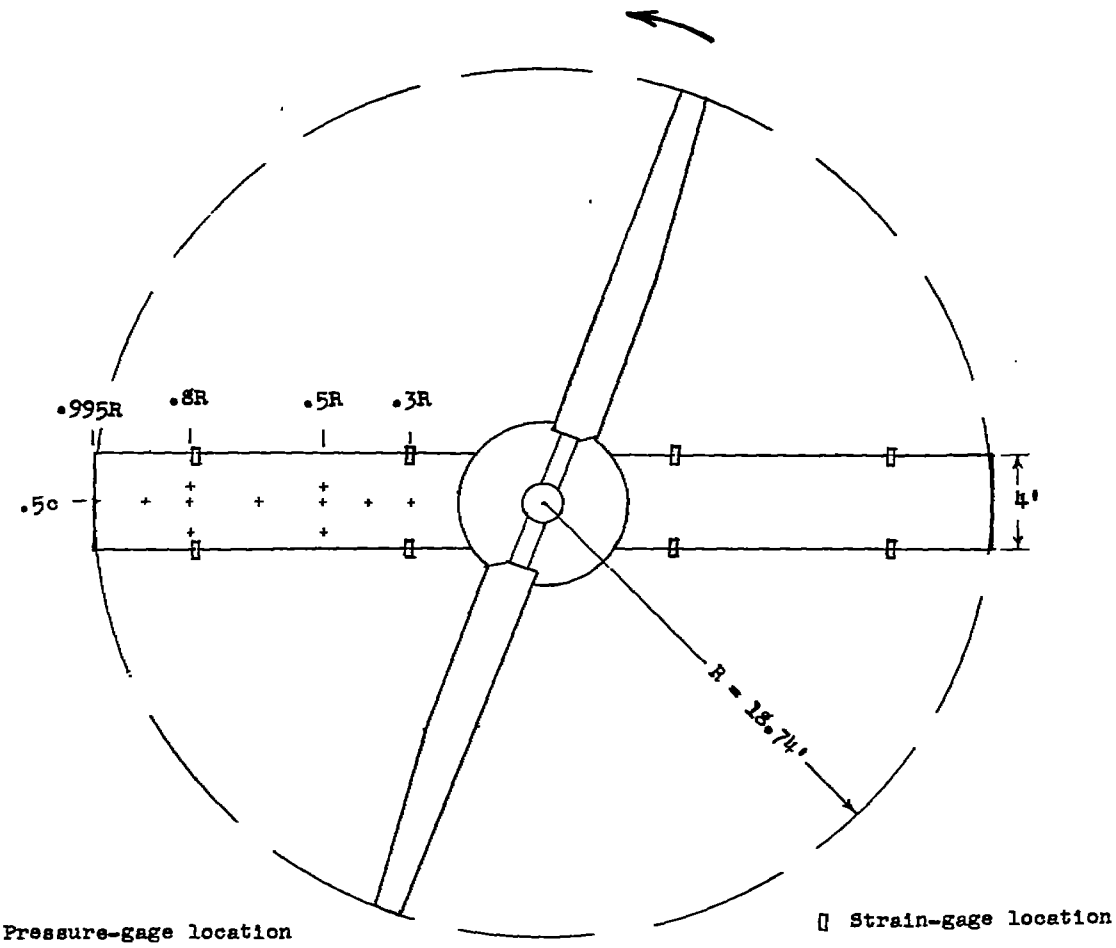

Figure 2.- Plan-form sketch of rotor and panels on the Langley helicopter test tower.

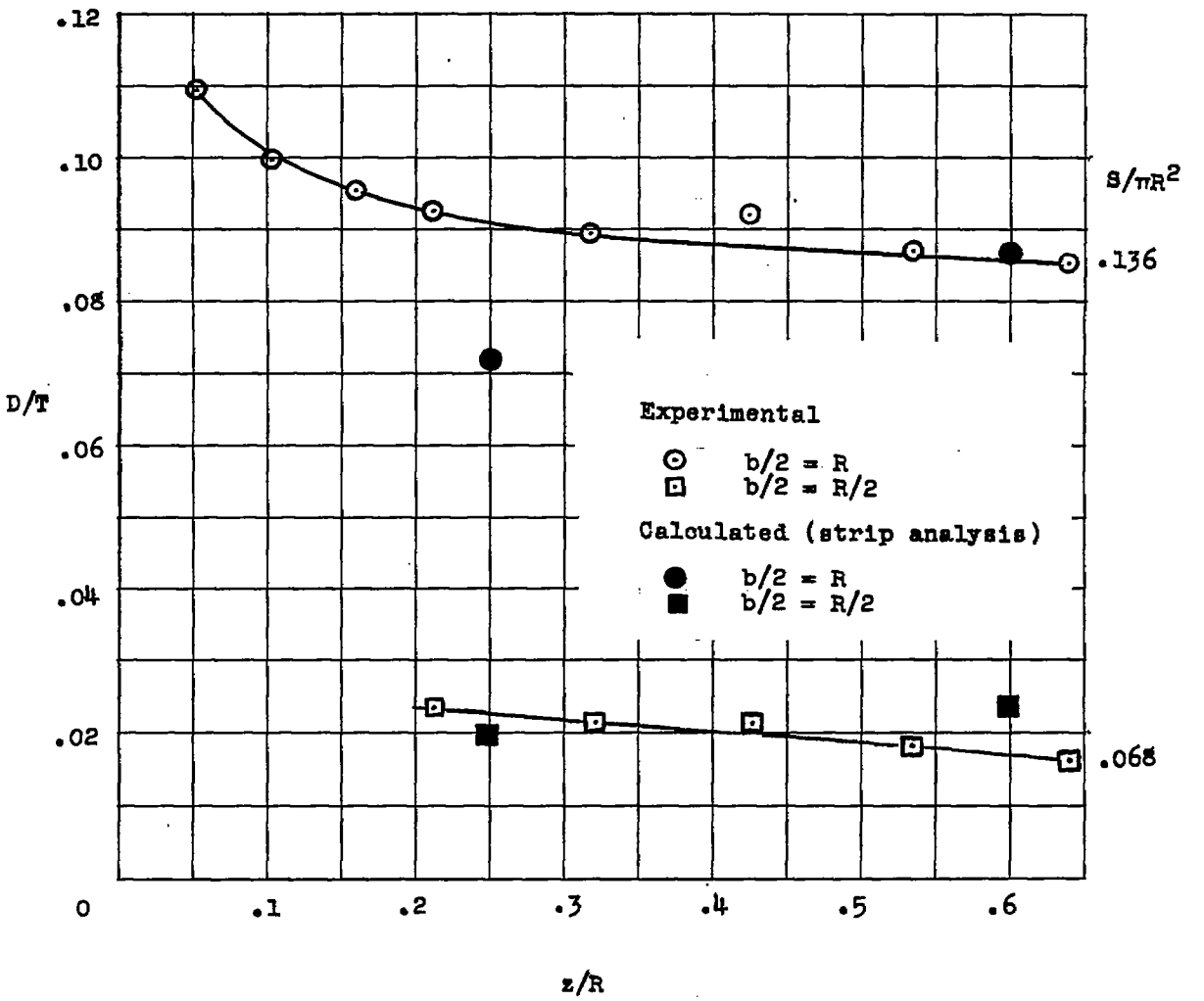

Figure 3.- The ratio of vertical drag to rotor thrust as function of distance beneath rotor plane of zero flapping.

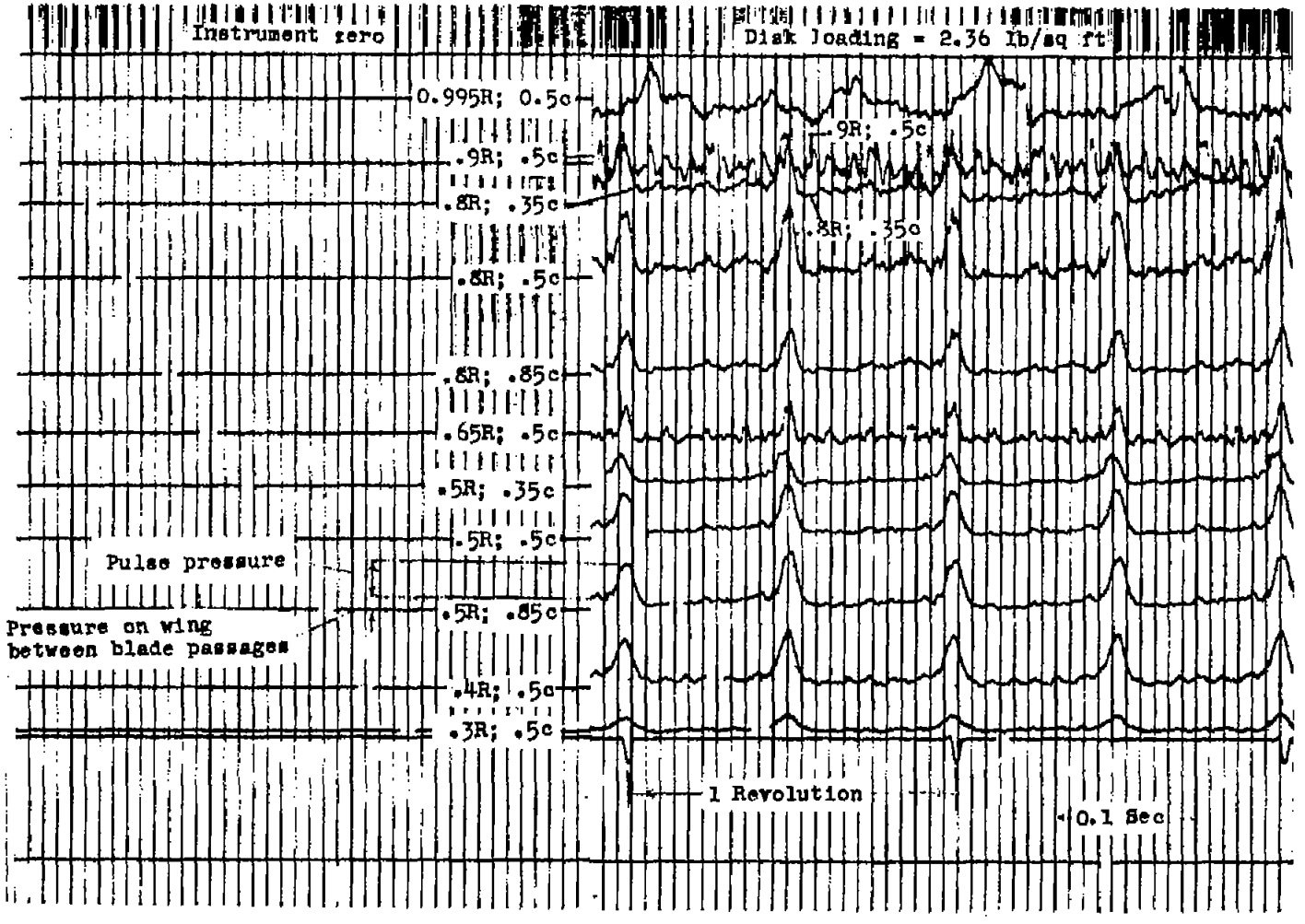

(a) Differential pressure; z/R = 0.053.

Figure 4.- Oscillograph record of pressure distribution on panel.

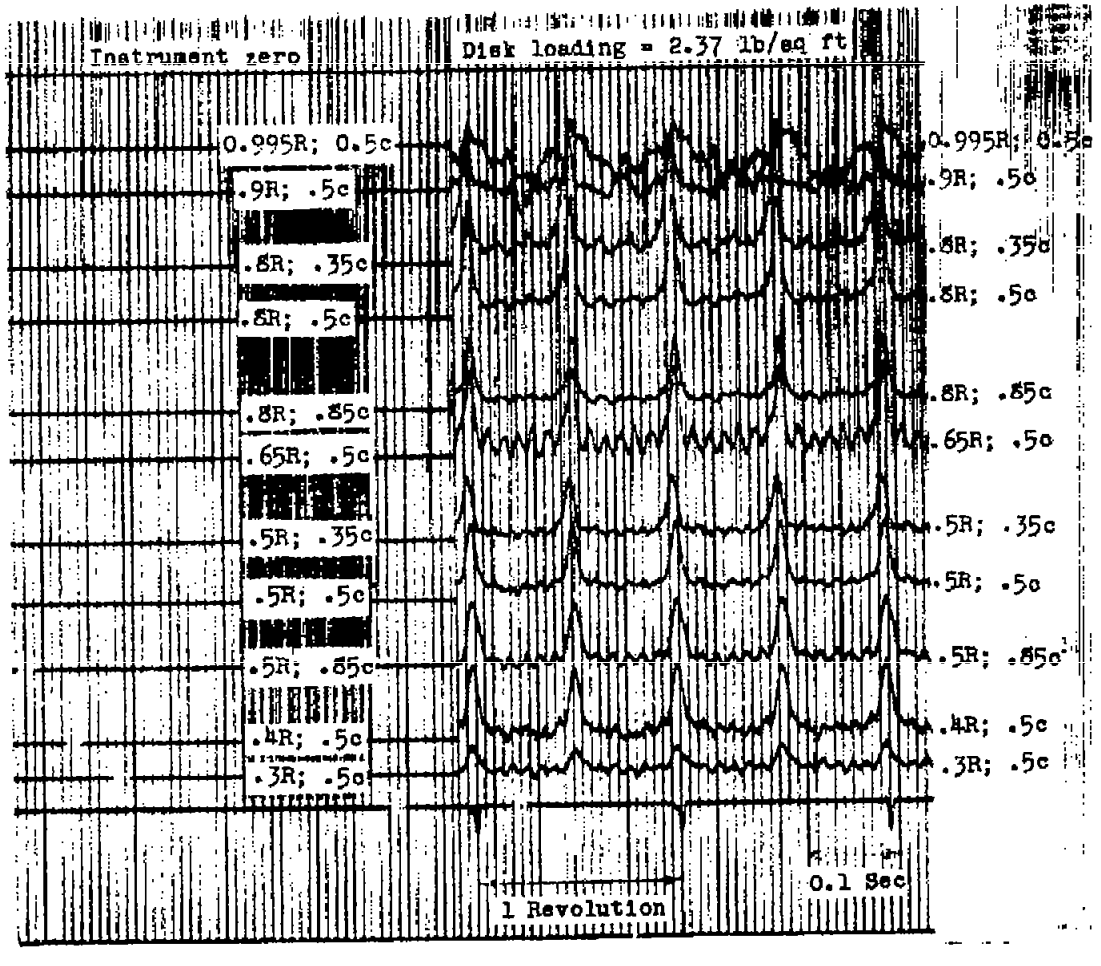

(b) Referenced to undisturbed atmospheric pressure; z/R = 0.053.

Figure 4.- Continued.

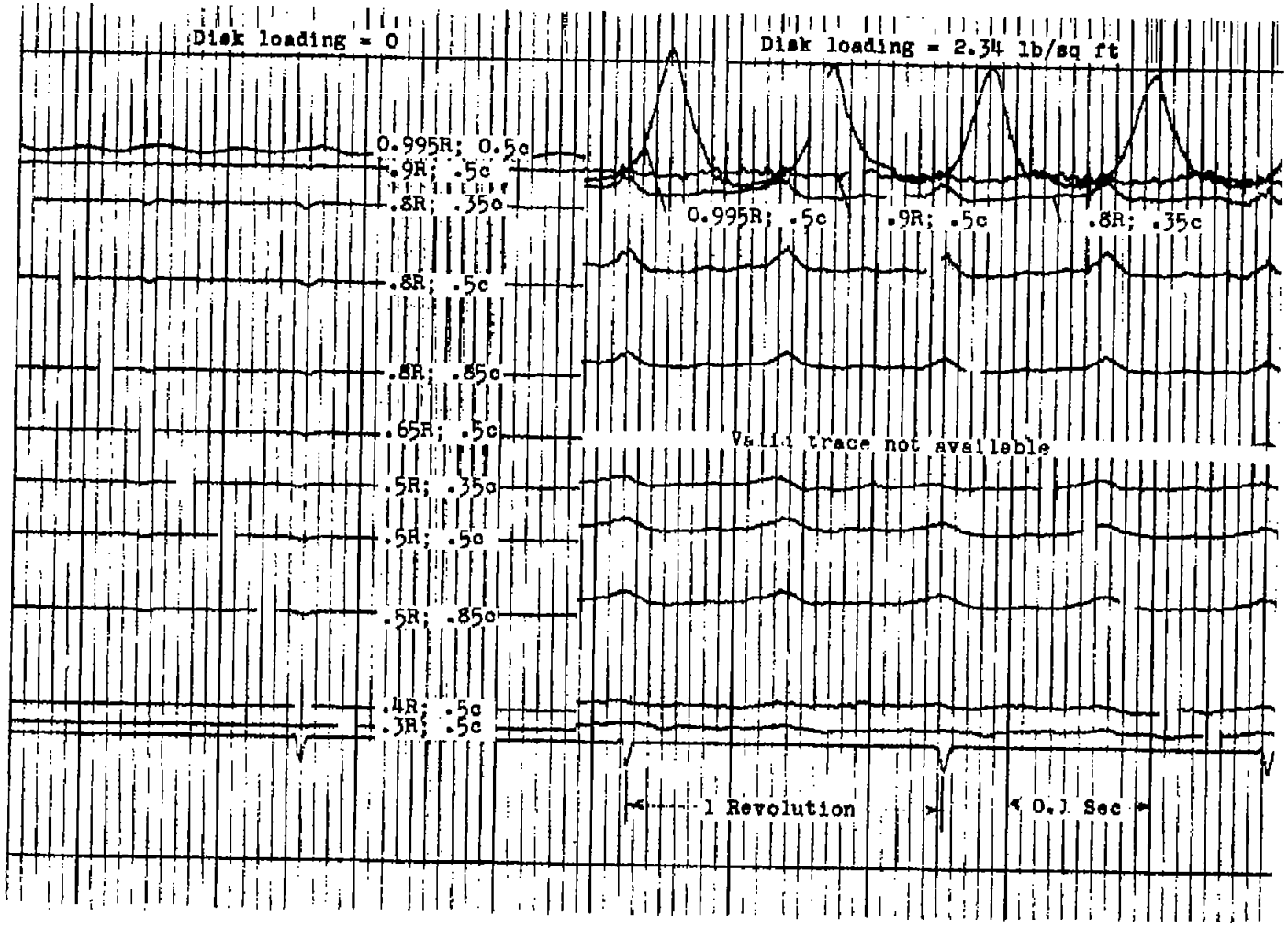

(c) Differential pressure; z/R = 0.214.

Figure 4.- Continued.

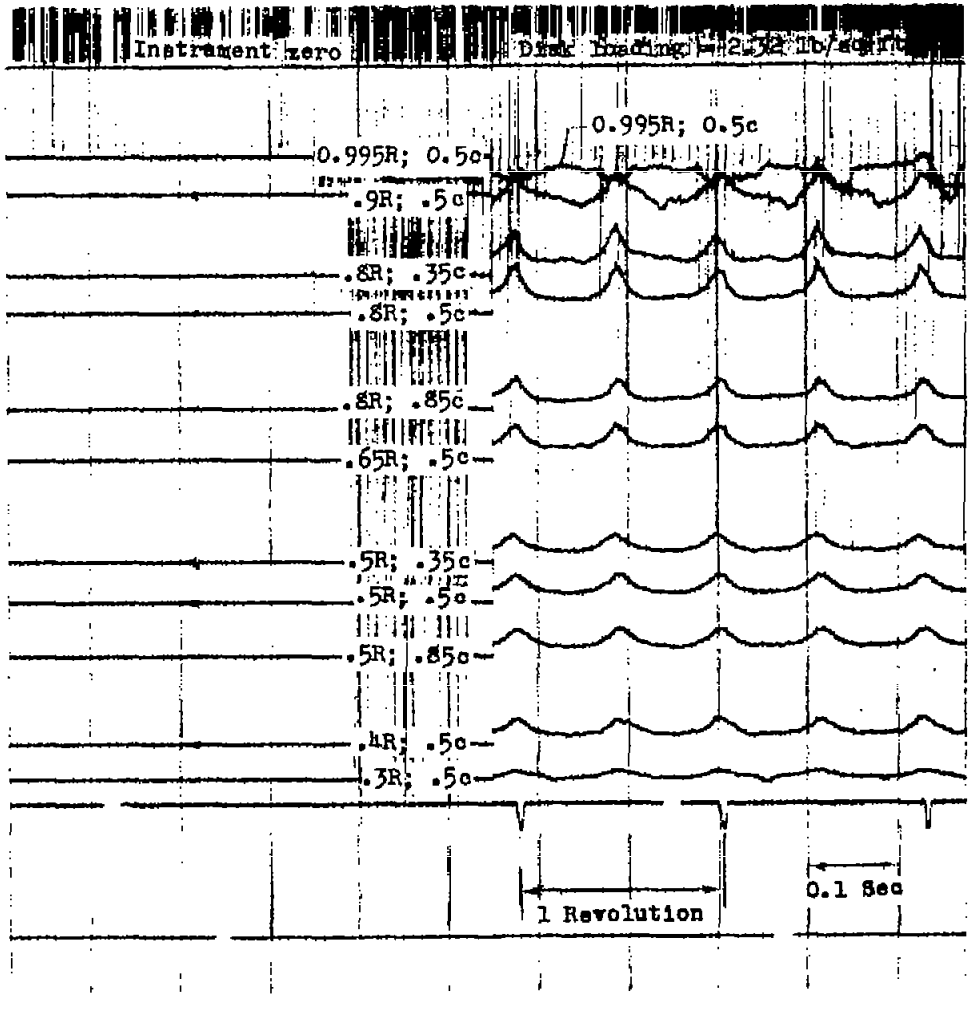

(d) Referenced to undisturbed atmospheric pressure; z/R = 0.214.

Figure 4.- Continued.

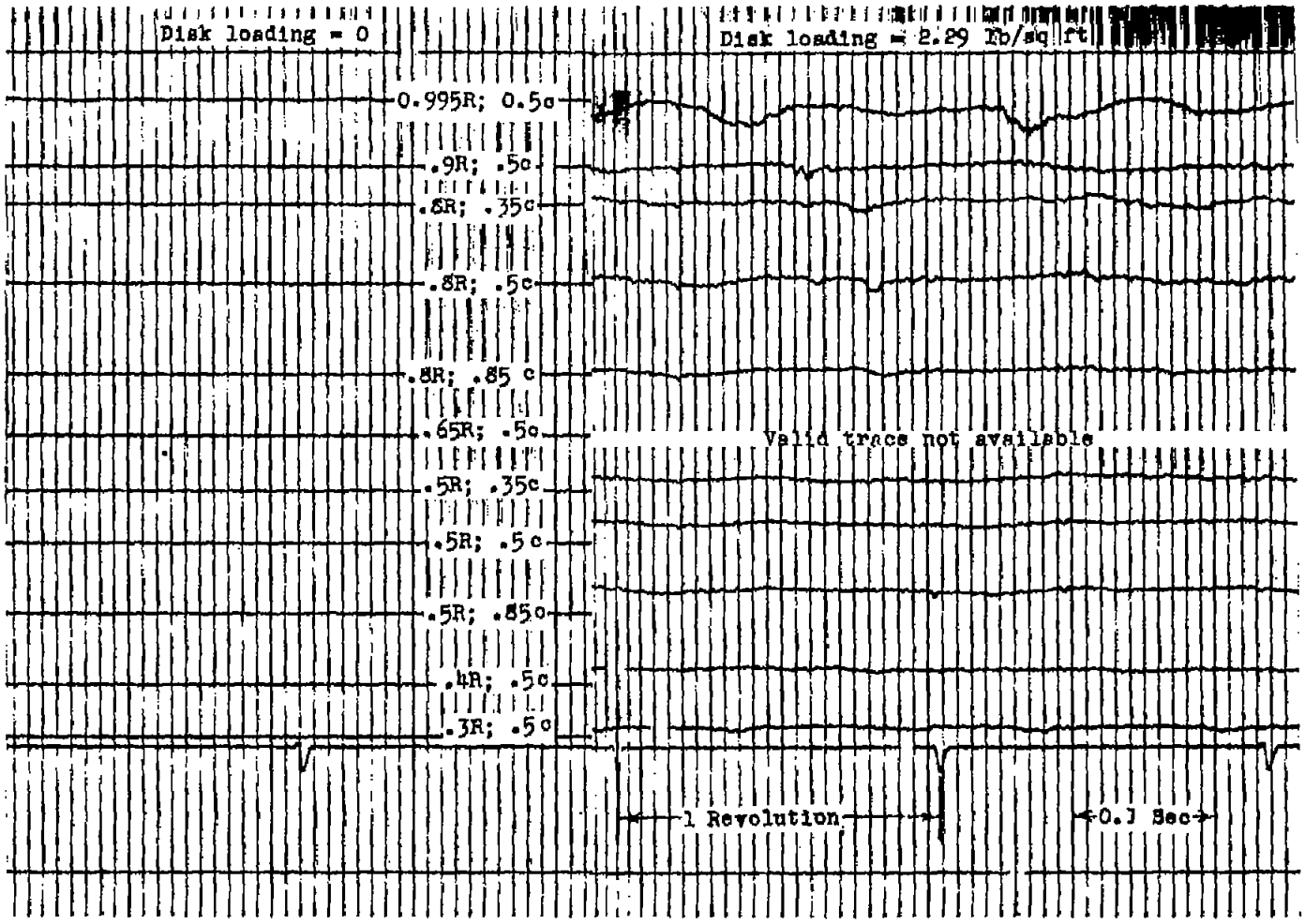

(e) Differential pressure; z/R = 0.64.

Figure 4.- Continued.

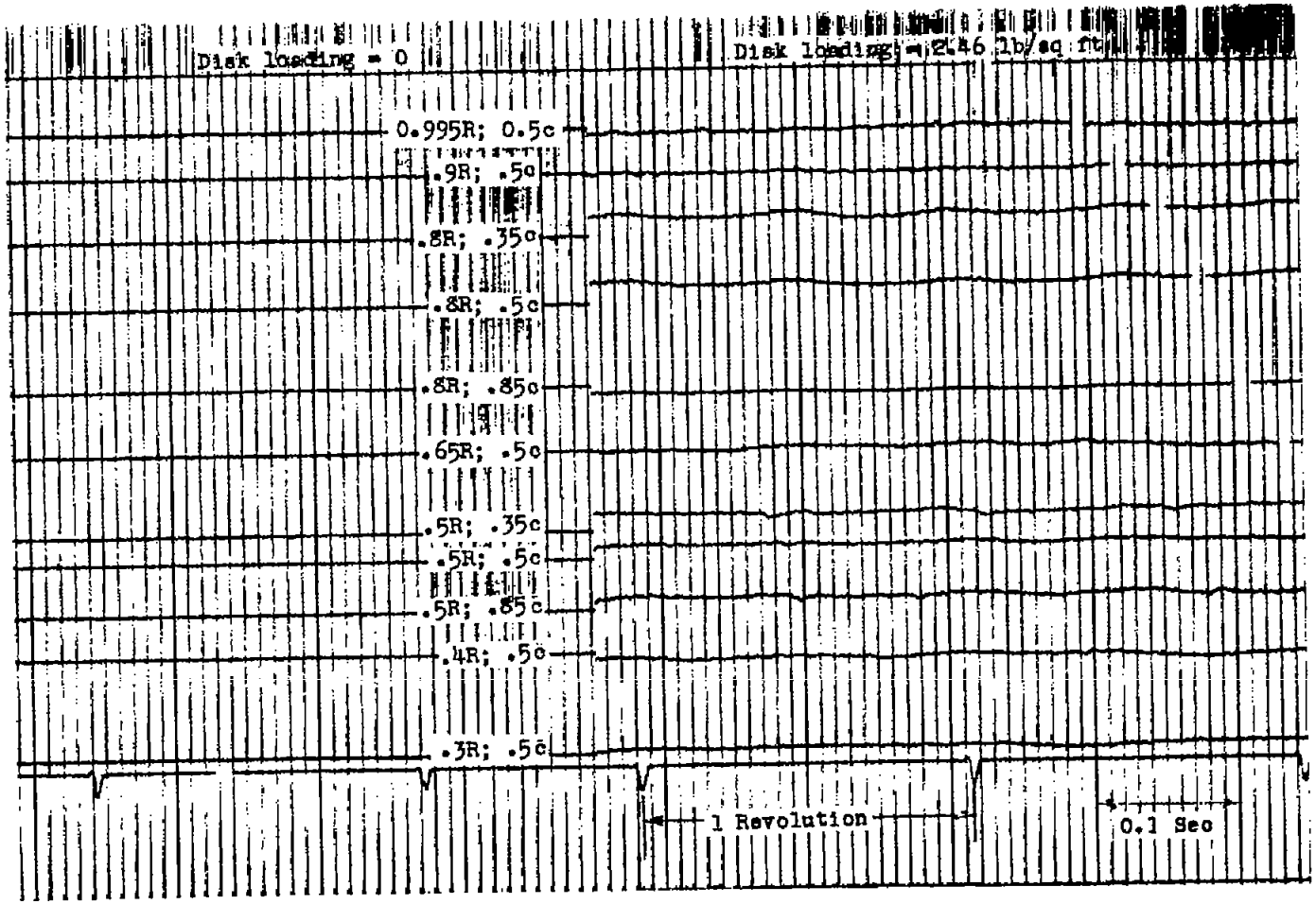

(f) Referenced to undisturbed atmospheric pressure; z/R = 0.64.

Figure 4.- Concluded.

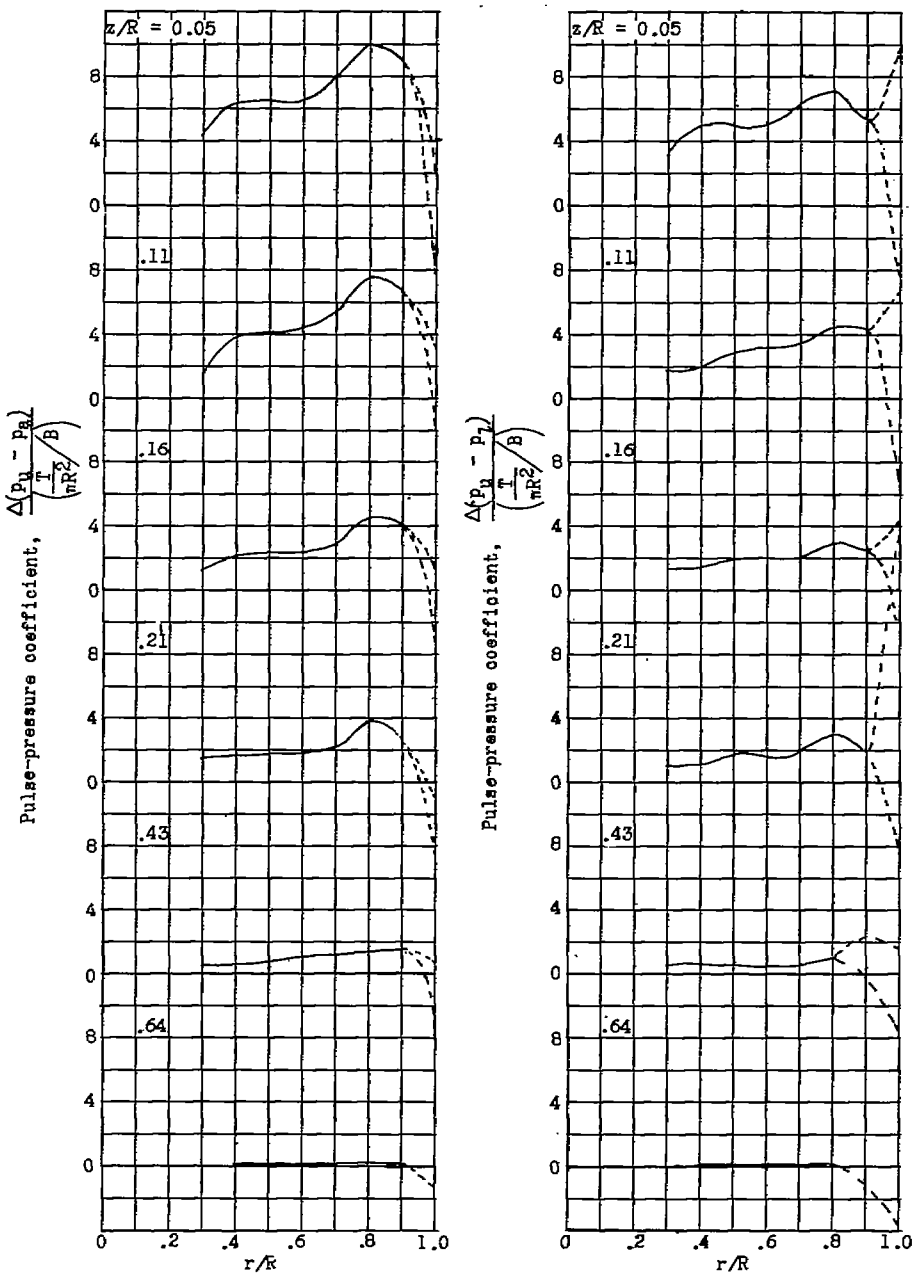

(a) Referenced to undisturbed atmospheric pressure.

(b) Differential pressure.

Figure 5.- Spanwise variation of pulse-pressure coefficient for various positions of flat panel beneath the rotor plane of zero flapping; rotor solidity = 0.027.

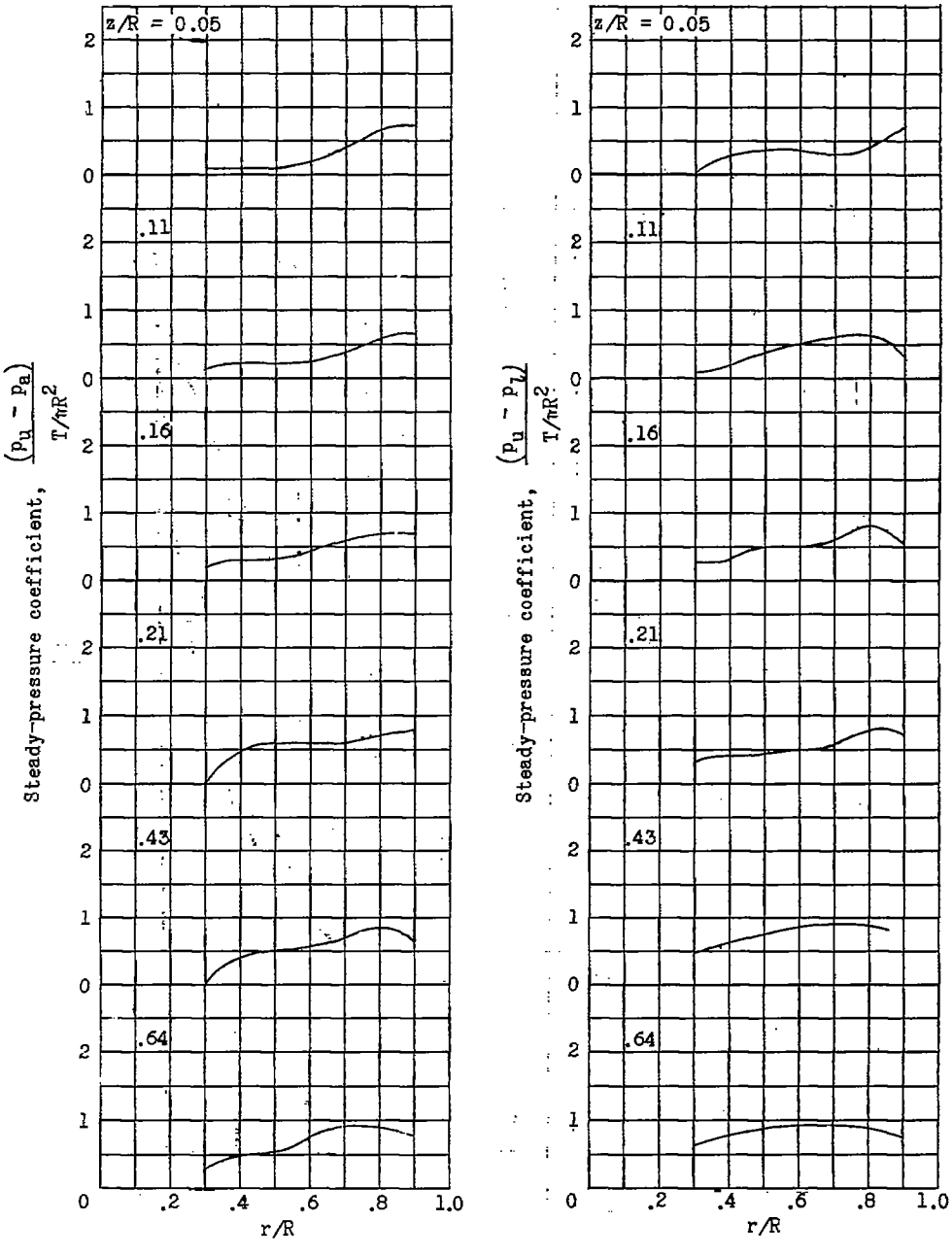

(a) Referenced to undisturbed atmospheric pressure.

(b) Differential pressure.

Figure 6.- Spanwise variation of steady-pressure coefficient for various distances of flat panel beneath rotor plane of zero flapping.

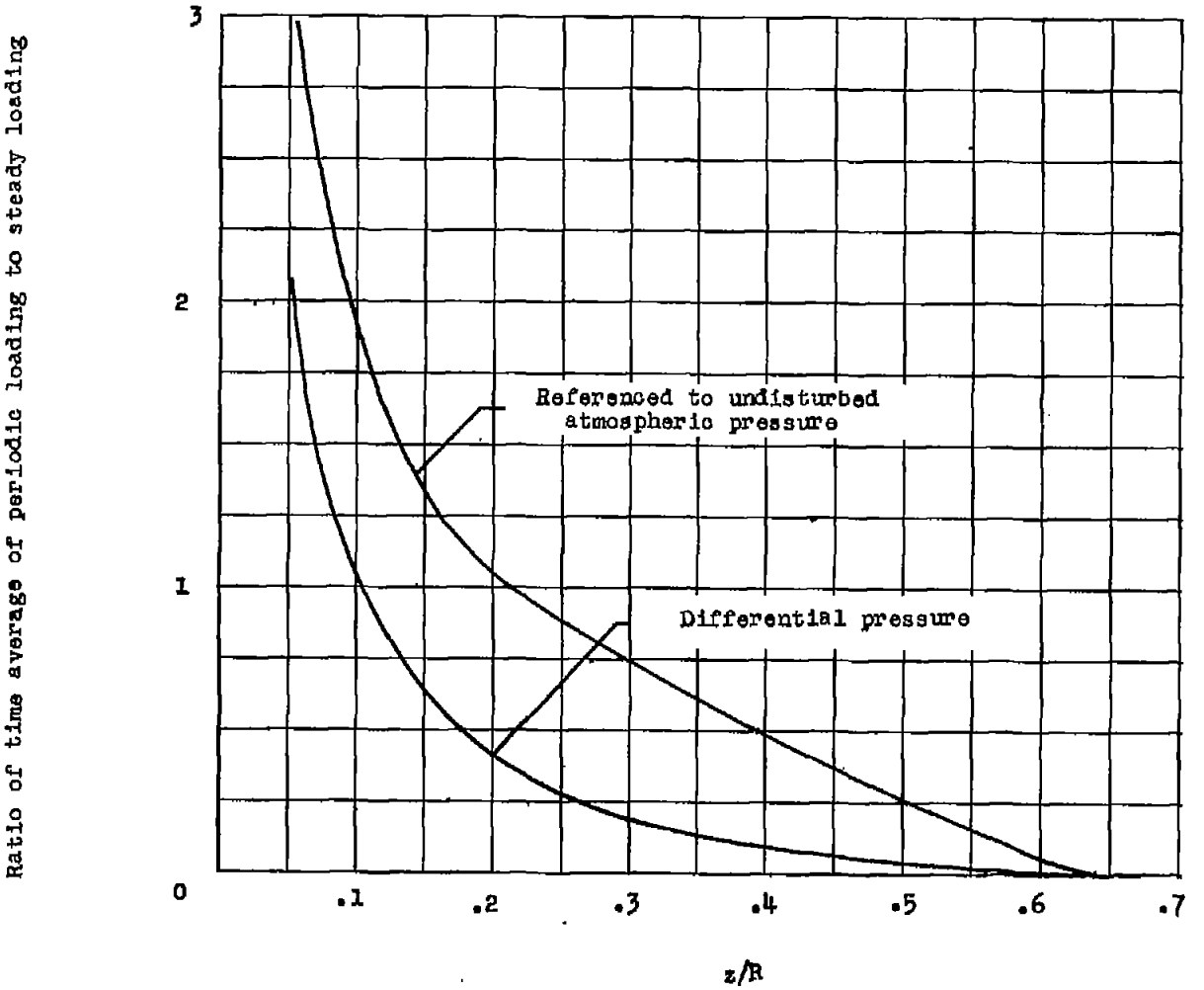

Figure 7.- Ratio of time average of periodic air loading to steady air loading (averaged over spanwise stations for 0.3R to 0.9R) as function of distance beneath plane of zero flapping.